A strategy to eliminate all nonlinear effects in constant-voltage hot-wire anemometry

Arganthaël Berson,[1] Philippe Blanc-Benon,[2] and Geneviève Comte-Bellot[2]
[1]*Queen's-RMC Fuel Cell Research Centre, Queen's University, 945 Princess Street, Kingston, Ontario K7L 5L9, Canada*
[2]*Laboratoire de Mécanique des Fluides et d'Acoustique, UMR CNRS 5509, École Centrale de Lyon, 36 avenue Guy de Collongue, 69134 Ecully Cedex, France*

(Received 29 September 2008; accepted 3 March 2009; published online 10 April 2009)

A constant-voltage anemometer is subject to nonlinear effects when the operating hot wire is exposed to large velocity fluctuations in the incident flow. This results in the generation of undesirable higher harmonics, just as in the two classic systems, constant-current and constant-temperature anemometers, for which no attempts are normally made to correct the nonlinearities. The present investigation shows that these undesirable higher harmonics can be suppressed in the case of a constant-voltage anemometer. A new approach to process experimental data is proposed. It is based on three explicit equations established and solved with all terms included, i.e., without linearization. These are (1) the first-order differential equation that describes the electronic circuit of a constant-voltage anemometer—this equation permits to deduce the instantaneous resistance of the hot wire from the output voltage of the anemometer; (2) the first-order differential equation that expresses the thermal lag behavior of the hot wire when used in a constant-voltage mode—this equation permits to restore the instantaneous resistance that an ideal wire would have without thermal inertia in the same flow conditions; and (3) the algebraic relation that expresses the heat-transfer law of an ideal wire, according to King's law, a look-up table, or a polynomial fit—this relation permits to deduce the instantaneous flow velocity from the instantaneous resistance of the ideal wire. The proposed method is easily implemented on a personal computer and permits odd turbulence moments, such as skewness factors, to be obtained satisfactorily. © *2009 American Institute of Physics.* [DOI: 10.1063/1.3103948]

I. INTRODUCTION

The effects of large-amplitude fluctuations in hot-wire anemometry have been investigated in the past for the most common systems, namely, the constant-current anemometer (CCA) and the constant-temperature anemometer (CTA). However, these effects have been left aside since then, although advanced data acquisition and processing systems could have been of great help to correct the nonlinearities.

A hot wire experiences thermal inertia, i.e., it does not respond to a change in excitation instantaneously but with some thermal lag. The wire operated in a CCA behaves as a first-order system. For small-amplitude fluctuations, the linearized governing equation of the CCA shows that thermal inertia attenuates the output signal and introduces a phase lag. Therefore, in commercial and homemade CCAs, thermal inertia is corrected by amplifying the ac part of the output signal with a gain and a phase lead increasing with frequency. Nevertheless, such correction is inaccurate for high-amplitude velocity fluctuations. Indeed, Corrsin[1] demonstrated that because the exact differential equation governing the response of the wire is of first order with time-dependent coefficients, the system experiences parametric excitation and higher harmonics are generated in the output signal. The linear correction procedure compensates for these harmonics as if they were turbulence. Resulting errors were analyzed by Corrsin[1] using Fourier series and Comte-Bellot and Schon[2] using an analog computer. Although they have a low energy content, these higher harmonics affect odd moments, especially the third moment, also called skewness factor, because of cross products between the fundamental and the harmonic contributions, e.g., for sinusoidal perturbations around 25%, a skewness factor around -0.30 is measured instead of zero.

Similar behavior affects the response of CTAs. It is commonly assumed that the instantaneous resistance of the wire in CTA is constant, provided that the frequency response of the system is sufficiently high. The usual practice is to digitize the bridge output and directly convert the instantaneous voltage output into instantaneous velocity using calibration curves. However, Freymuth[3,4] demonstrated that as with any other hot-wire anemometer, the CTA experiences thermal inertia. The response of the wire is governed by a third-order differential equation with time-dependent coefficients deriving from the coupling between the heat-transfer law of the wire, the bridge circuit, and the properties of the feedback amplifier. For large-amplitude velocity fluctuations, Freymuth showed that at least a second harmonic is generated at the bridge output. This harmonic is expected to be maximum around half of the cutoff frequency of a typical system with an amplitude relative to the fundamental around 10%.[4] As a consequence, if the uncorrected CTA output, which includes this second harmonic, is directly converted into velocity using the calibration curves of the CTA, the

resulting velocity signal will also contain the contribution of the second harmonic, which is erroneous. For instance, in their study of the kinetic energy budget of turbulence in a high-Reynolds number jet, a budget that involves third-order moments and other cross products, Hussein *et al.*[5] reported discrepancies between the results obtained with a fixed hot wire and those obtained with a flying hot wire and laser-Doppler anemometry. It is most likely that these discrepancies resulted from high turbulence levels experienced by the fixed hot wire when close to the free edges of the jet.

Furthermore, the bandwidth of the CTA is not constant. The coefficients of the governing equation of the CTA are usually tuned using a square-wave test so as to achieve an optimal response for a given operating point.[6] Away from this operating point, the bridge is unbalanced, which affects the frequency response of the system and enhances nonlinearities. In flows with large-amplitude velocity fluctuations, this generates dynamic errors and may even lead to unstable operation of the CTA. Ligęza[7] proposed a modified CTA with a constant bandwidth. However, for commercial CTAs, the governing equation being rather complicated, with coefficients that are not always accurately known, a software procedure for correcting thermal inertia would not be straightforward.

For the constant-voltage anemometer (CVA) recently patented by Sarma,[8] Comte-Bellot[9,10] showed that the wire thermal lag also leads to a differential equation exhibiting *parametric excitation*, but, with the exception of one preliminary study,[11] no explicit treatment has been undertaken. So far, studies have focused on small-amplitude fluctuations and have pointed out several interesting features of the CVA. For example, using the software correction of thermal inertia developed by Sarma *et al.*,[12] the CVA bandwidth remains constant, and experiments in difficult conditions, such as in supersonic boundary layers,[13] shock waves,[14] or flight tests,[15] are facilitated. However, these investigations were restricted to the study of turbulence levels, spectra, and double correlations. If one desires to extend the use of the CVA toward the investigation of higher moments, such as those of the third order, which express the convection of turbulent kinetic energy by turbulent fluctuations, the linear approach is obviously not sufficient as cross products between fundamental and harmonics may lead to systematic errors.

In the present work, all the equations of the CVA are revisited. The first objective is to analyze the different sources of nonlinearity. The second and more important objective is to develop a strategy to process experimental data so as to eliminate all nonlinear effects.

The paper is organized as follows. The full basic equations that govern the wire response and the CVA circuit are presented in Sec. II and their linearized forms are summarized in Sec. III. The nonlinearities that appear along the entire path, from the input velocity to the CVA output voltage, are analyzed in Sec. IV for sinusoidal velocity perturbations having different amplitudes and frequencies. Section V reviews the previous method used to process experimental data, a method that mostly relies on linearized equations. Section VI describes the present strategy, which is based on full equations. Section VII compares the two methods for sinusoidal velocity perturbations and realistic turbulent velocities provided by large eddy simulation in a high speed jet. In Section VIII, some conclusions regarding the easy implementation of the present strategy are listed.

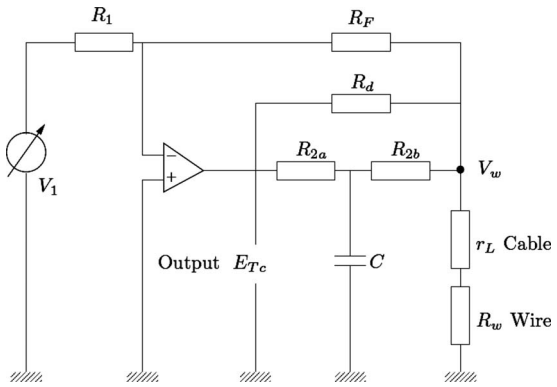

FIG. 1. Schematic drawing of a CVA.

II. BASIC EQUATIONS OF A CVA

Three equations are to be considered to describe all nonlinear effects. They deal with the CVA circuit, the thermal inertia of the wire, and the calibration law.

A. CVA circuit

The transfer function that relates the resistance R_w of the real hot wire to the output voltage E_{T_c} of the CVA has been established by Sarma[8] and by Comte-Bellot *et al.*[16] who included the resistance r_L of the cable that connects the hot wire to the anemometer. With the notations indicated in Fig. 1 for the CVA circuit, this basic equation is

$$E_{T_c} = V_w \left[1 + \frac{R_2}{R_F} + \frac{R_2}{R_w + r_L} + T_c R_2 \frac{d}{dt}\left(\frac{1}{R_w + r_L} \right) \right]. \quad (1)$$

The notation E_{T_c} indicates that the CVA output voltage corresponds to a selected value of the time constant T_c in the hardware compensation circuit of the CVA, where

$$T_c = \frac{R_{2a} R_{2b}}{R_2} C.$$

T_c is adjusted by capacitance C and resistances R_{2a} and R_{2b} with $R_{2a}+R_{2b}=R_2$. T_c is set to provide a partial compensation to the thermal inertia of the hot wire. An important feature of this procedure is that a constant bandwidth is obtained[12] when T_c is unchanged during the tests. Often T_c is set to 100 μs. It is also worth adding that E_{T_c} is large because most of the current heating the wire flows through resistance R_2, which is itself large, $R_2=100\ \Omega$. The voltage across the wire and its lead, $V_w=(R_w+r_L)I_w$, is maintained constant independently by the upper branch of the circuit in Fig. 1 since $V_w=V_1 R_1/R_F$ with $R_1=100\ \Omega$ and $R_F=400\ \Omega$.

In Eq. (1), note that the inverse of the wire resistance $(1/R_w)$ appears. This may constitute a source of nonlinearity that has to be considered at large-amplitude changes.

B. Hot-wire thermal inertia

The comparison between the resistance R_w of a real hot wire with thermal lag and the resistance R_w^* of an ideal hot wire without thermal lag has been established by Comte-Bellot,[9] neglecting the cable connecting the hot-wire probe to the anemometer, and by Comte-Bellot *et al.*[16] when the cable is taken into account with its resistance r_L. With the following condition imposed by the CVA,

$$V_w = (R_w + r_L)I_w = (R_w^* + r_L)I_w^* = \text{a constant}, \tag{2}$$

the comparison makes use of two basic heat-transfer balances

$$0 = V_w^2 \frac{R_w^*}{(R_w^* + r_L)^2} - (R_w^* - R_a)f(U), \tag{3}$$

$$\frac{m_w c_w}{\chi R_0}\frac{dR_w}{dt} = V_w^2 \frac{R_w}{(R_w + r_L)^2} - (R_w - R_a)f(U). \tag{4}$$

Equation (3) is for an ideal wire without thermal lag. At any time, the Joule energy in the wire is balanced by the energy lost into the flow by forced convection. Equation (4) is for a real wire in which the difference between the energy due to Joule heating and the energy lost by forced convection is stored in the wire and creates a thermal lag in the transmitted signal. $f(U)$ is a function of the fluid velocity U normal to the wires, e.g., $f(U)=A+B\sqrt{U}$ in King's law, and heat loss toward the supports is neglected.

Eliminating $f(U)$ between Eqs. (3) and (4) gives

$$\frac{1}{V_w^2}\frac{m_w c_w}{\chi R_0}\frac{dR_w}{dt} = \frac{R_w}{(R_w + r_L)^2} - \frac{R_w^*}{(R_w^* + r_L)^2}\frac{R_w - R_a}{R_w^* - R_a}. \tag{5}$$

This equation has several coefficients that are time dependent and parametric excitation affects its solution. Therefore, assuming a single-frequency excitation of R_w^*, higher harmonics may appear in R_w and their consequences on further signal processing have to be considered.

C. Heat-transfer law

Among the many heat-transfer laws available in the literature to relate the resistance R_w^* of an ideal wire to the incident flow velocity U, King's law is of common use in subsonic flows, and Dewey's approach using Nusselt and Reynolds numbers is most appropriate to supersonic flows.[10] The canonical form of King's law is

$$\frac{R_w^* I_w^2}{R_w^* - R_a} = A + B\sqrt{U}, \tag{6}$$

with A and B approximately constant.[10] Clearly R_w^* is not linearly related to U. This is well known, but let us stress that any wire has these harmonics embedded in the signal it delivers.

III. LINEARIZED APPROXIMATE EQUATIONS

The linearization of Eqs. (1), (5), and (6) provides useful hints for the understanding of the CVA and will serve as reference for the developments made in Sec. V. Splitting every instantaneous quantity

$$U = \bar{U} + u' \quad \text{with} \quad u' \ll \bar{U},$$

$$R_w^* = \bar{R}_w^* + r_w'^* \quad \text{with} \quad r_w'^* \ll \bar{R}_w^*,$$

$$R_w = \bar{R}_w + r_w' \quad \text{with} \quad r_w' \ll \bar{R}_w,$$

$$E_{T_c} = \bar{E}_{T_c} + e'_{T_c} \quad \text{with} \quad e'_{T_c} \ll \bar{E}_{T_c},$$

and substituting into Eqs. (1), (5), and (6) give

$$e_s' = -V_w \frac{R_2}{(\bar{R}_w + r_L)^2}\left(r_w' + T_c\frac{dr_w'}{dt}\right), \tag{7}$$

$$M_w^{\mathrm{CVA}}\frac{dr_w'}{dt} + r_w' = r_w'^*, \tag{8}$$

$$\frac{r_w'^*}{\bar{R}_w^*} = -\frac{\bar{a}_w}{2(1+\bar{a}_w)}\frac{B\sqrt{\bar{U}}}{A + B\sqrt{\bar{U}}}\frac{u'}{\bar{U}}. \tag{9}$$

Although limited to small-amplitude perturbations, this linear approach exhibits two interesting features of the CVA:

(i) The coefficient of dr_w'/dt in Eq. (8) is the time constant M_w^{CVA} of the wire when V_w=a constant. According to the linear approach,[16] its expression is

$$M_w^{\mathrm{CVA}} = \frac{1}{V_w^2}\frac{m_w c_w}{\chi R_0}(\bar{R}_w + r_L)^2\frac{\bar{a}_w}{1+2\bar{a}_w} \times LM \quad . \tag{10}$$

The factor LM comes from the connecting cable

$$LM = \left[1 + \frac{r_L}{R_a(1+\bar{a}_w)}\right]\left[1 + \frac{r_L}{R_a(1+\bar{a}_w)(1+2\bar{a}_w)}\right]^{-1}, \tag{11}$$

for example, $LM \simeq 1.1$ when $R_a=3.8\ \Omega$, $\bar{a}_w=0.80$, and $r_L=1\ \Omega$.

(ii) The comparison between Eqs. (8) and (7) clearly shows that the output signal e'_{T_c} is already partly corrected by T_c for the thermal lag.

IV. ANALYSIS OF NONLINEARITIES

Nonlinearities occur along the whole path from the incident velocity U to the CVA output voltage E_{T_c} by the cumulative effect of Eqs. (6), (5), and (1) taken in this order, as shown below,

$$U \Rightarrow R_w^* \Rightarrow R_w \Rightarrow E_{T_c}.$$

Their trace is therefore interesting to follow. A sinusoidal velocity input is chosen of the form

$$U = U_0 + u_1\sqrt{2}\sin 2\pi f_e t,$$

with $U_0=50\ \mathrm{m\ s^{-1}}$ and u_1 in the range of $0-12.5\ \mathrm{m\ s^{-1}}$ corresponding to a turbulence level up to 25%. A 1.25 mm long tungsten wire, 5 μm in diameter, i.e., with typical characteristics for turbulence investigations, is chosen. Hence, $R_a \simeq 3.8\ \Omega$. For the cable and wire supports, $r_L \simeq 1\ \Omega$. The operating parameters are chosen at $U=U_0$: $a_w=0.80$, hence $R_w \simeq 6.8\ \Omega$, $M_w^{\mathrm{CVA}}=220\ \mu\mathrm{s}$, and $V_w=605$ mV. Afterward,

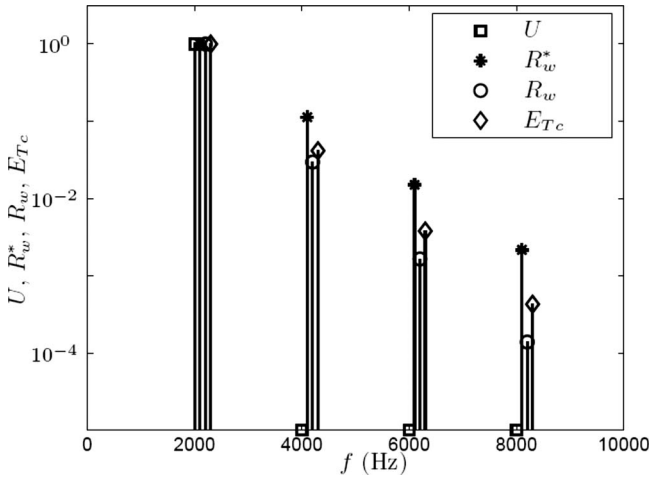

FIG. 2. Harmonic contents of signals along the path $U \Rightarrow E_{T_c}$ for a sinusoidal velocity input, 25% turbulence level. For the sake of readability, all the quantities are normalized by their amplitude at fundamental frequency and their spectra are shifted by a few hertz so that they do not overlap.

this V_w value is kept constant by the CVA circuit when U varies. The excitation frequency f_e is adjustable in the range of 100–5000 Hz, which, in terms of $2\pi f_e M_w^{\mathrm{CVA}}$, covers a significant range from 0.13 to 6.40. Other values of interest are $\chi = 0.0045\ \mathrm{K}^{-1}$ and $c_w = 140\ \mathrm{J\,kg^{-1}\,K^{-1}}$. All equations are solved using MATLAB 7.4. Time derivatives are approached by a first-order upwind finite difference scheme. The sampling frequency is $f_s = 100 f_e$. In all data sets, the first five samples are suppressed to remove the transient effect of initial conditions when solving the differential equations.

The harmonic contents of the transmitted signals are displayed in Fig. 2 at each step of the path for a sunusoidal velocity input at $f_e = 2000$ Hz and a turbulence level of 25%. Figure 2 shows the importance of the first step $U \Rightarrow R_w^*$, which creates a second harmonic whose relative amplitude is around 0.10 and higher harmonics with slowly decreasing amplitudes. All these harmonics are then interacting in the two other steps $R_w^* \Rightarrow R_w$ and $R_w \Rightarrow E_{T_c}$, governed by differential equations with time-dependent coefficients. Relative phases are also involved. They may be easily computed, but for the sake of clarity, the study of skewness factors is preferred. For a signal $x(t)$, a skewness factor is defined by $S_x = \overline{x^3}/(\overline{x^2})^{3/2}$, overlined quantities being time averaged. It involves triple cross products between all spectral components and constitutes a palpable indicator for nonlinear activity. The most significant of these triple cross products is of the form $3 \times \alpha_1^2 \sin^2(2\pi f_e t + \phi_1) \times \alpha_2 \sin(4\pi f_e t + \phi_2)$ between a fundamental and its second harmonic with amplitudes α_1 and α_2 and phases ϕ_1 and ϕ_2, respectively.

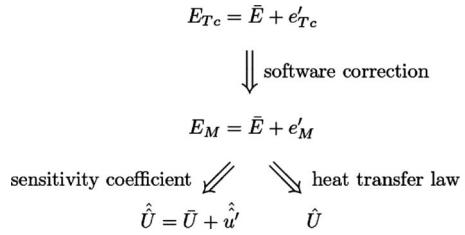

FIG. 3. Diagram of the previous method for data processing.

The skewness factors obtained at each step along the path $U \Rightarrow E_{T_c}$ are indicated in Table I for sinusoidal velocity inputs at different frequencies f_e and a fixed turbulence level of 25%. The skewness factor of U, which is zero, constitutes a reference. The skewness of R_w^* has a positive and constant value. It is due to the curvature of the heat transfer law, as simply observed with King's law, where the positive excursions of R_w^* are greater than the negative ones for a symmetrical velocity change around U_0. Of course, a hot wire transmits such a highly asymmetric signal. The skewness values of R_w, as well as those of E_{T_c}, show considerable spread. Some values are even illogical such as those at low frequency where nonlinear effects are expected to be minimal. Furthermore, for the skewness of E_{T_c}, a zero value is never obtained. This shows that the signal delivered straight from an anemometer cannot be used to obtain a skewness factor directly on the grounds that it is a dimensionless quantity. Again, this highlights the fact that the harmonics created at each step mix and interact in a complex manner. A well-planned procedure is clearly needed to process the CVA output E_{T_c} to fully recover a correct input velocity.

V. PREVIOUS METHOD FOR DATA PROCESSING

The method previously used for correcting the thermal inertia of the CVA is mostly based on the linearized expressions presented in Sec. III. The output voltage E_{T_c} is split into its dc and ac parts and the main steps of the processing are indicated in Fig. 3. Subscript T_c is for a signal compensated with T_c, subscript M is for a signal fully compensated with the measured M_w^{CVA}. For the dc part, the linearization gives $\bar{E}_{T_c} = \bar{E}_M$, simply noted as $\bar{E}$. The ac part is specifically processed by a software procedure. The software procedure

TABLE I. Skewness factors along the path $U \Rightarrow E_{T_c}$ for a sinusoidal velocity input, 25% turbulence level.

Frequency f_e (Hz)	$2\pi f_e M_w^{\mathrm{CVA}}$	Skewness U	Skewness R_w^*	Skewness R_w	Skewness E_{T_c}
100	0.13	0	0.2416	0.2298	−0.1796
250	0.32	0	0.2416	0.1899	−0.1481
500	0.64	0	0.2416	0.1359	−0.1102
1000	1.28	0	0.2416	0.0860	−0.0807
3000	3.84	0	0.2416	0.0321	−0.0905
5000	6.40	0	0.2416	0.0196	−0.0969

completes the compensation of the thermal lag from T_c to the time constant of the wire $M_w^{\mathrm{CVA}}(LM)^{-1}$. Obtaining e'_M from e'_{T_c} involves a numerical loop simply expressed in terms of a s-Laplace transform by

$$e'_M = e'_{T_c}\frac{1+M_w^{\mathrm{CVA}}LM^{-1}s}{1+T_c s}.$$

The method is detailed by Sarma *et al.*[12] or Comte-Bellot and Sarma.[13] M_w^{CVA} is readily measured using a square-wave signal and a special circuit developed by Sarma and Lankes.[17] The major advantage of a software correction is that all experimental data may be acquired using T_c without the need to adjust the R-C circuit at every test point. Data acquisition is therefore fast. Moreover, the bandwidth of the CVA is kept constant.[12]

Two variants were applied to this fully corrected e'_M signal. The first variant relies on a sensitivity coefficient, usually noted as S_u^{CVA} and derived from Eq. (9). A coefficient LS is also required to take into account resistances R_2 and R_F for the CVA circuit and resistance r_L for the connecting cable.[16] This gives

$$S_u^{\mathrm{CVA}} = \frac{\bar{a}_w}{2(1+2\bar{a}_w)}\frac{B\sqrt{U}}{A+B\sqrt{U}} \times LS, \tag{12}$$

with

$$LS = \left[1+\left(\frac{R_a}{R_2}+\frac{R_a}{R_F}\right)\left(1+\bar{a}_w+\frac{r_L}{R_a}\right)\right]^{-1} \times \left[1+\frac{r_L}{R_a(1+\bar{a}_w)(1+2\bar{a}_w)}\right]^{-1}.$$

A velocity fluctuation u', hereafter denoted by a double hat, is then deduced from $e'_M, \bar{E}, S_u^{\mathrm{CVA}}$, and $\bar{U}$,

$$\frac{\hat{\hat{u}}'}{\bar{U}} = [S_u^{\mathrm{CVA}}]^{-1}LS\frac{e'_M}{\bar{E}}. \tag{13}$$

For example, $S_u^{\mathrm{CVA}} \simeq 0.15$, $LS \simeq 0.95$ for $R_a = 3.8\ \Omega$, $\bar{a}_w = 0.80$, and $r_L = 1\ \Omega$. This method is generally adopted for supersonic flows for which fluid mechanics equations are often linearized to permit velocity, density, and temperature fluctuations to be considered jointly.[10,18–20] Also, investigations focus on turbulence levels, spectra, and double correlations.

The second variant makes use of a reconstructed dc +ac signal, $\hat{E}_M = \bar{E} + e'_M$, hereafter denoted by a single hat. Then, $\hat{R}_w$ is obtained from $\hat{E}_M$ and introduced into a heat transfer law, such as King's law, to obtain the velocity $\hat{U}$. In fact, this latter variant has been developed by Sarma and Comte-Bellot[21] to take into account drifts in the incident flow temperature T_a using one wire only, since V_w can be externally changed rapidly in a CVA, thus operating the wire in heated and cold resistance modes.

Table II indicates the skewness factors obtained by these two variants for a sinusoidal velocity input, 25% turbulence level, and different frequencies f_e. Clearly, the skewness of $\hat{\hat{u}}'$ suffers from the same drawbacks as the skewness of E_M, since the sensitivity coefficient imposes a linear connection between the two signals. The skewness of $\hat{U}$ has a correct trend with frequency f_e, i.e., its values tend toward zero when f_e decreases. This is made possible because the higher harmonics inherent in the heat-transfer law, as seen by the wire, are taken into account by the use of the same curve during data processing rather than its tangent at the operating point. However, at high frequencies, the zero value expected for a sinusoidal signal is not obtained and a value of around 0.08 remains. Regarding amplitude levels, very satisfying results are obtained regardless of the variant used, errors being less than 1%.

TABLE II. Comparison of the two variants used in previous data processing for a sinusoidal velocity input, 25% turbulence level.

$2\pi f_e M_w^{\mathrm{CVA}}$	Skewness E_{T_c}	Skewness E_M	Skewness $\hat{\hat{u}}'$	Skewness $\hat{U}$
0.13	−0.1796	−0.1833	−0.1833	0.0173
0.32	−0.1481	−0.1612	−0.1612	0.0363
0.64	−0.1102	−0.1279	−0.1279	0.0661
1.28	−0.0807	−0.1020	−0.1020	0.0873
3.84	−0.0905	−0.0999	−0.0999	0.0848
6.40	−0.0969	−0.1012	−0.1012	0.0829

VI. PRESENT METHOD FOR DATA PROCESSING

In the present method, the path responsible for harmonic generation is exactly inverted, as depicted in Fig. 4. Note that contrary to the previous method described in Sec. V, which requires that the dc and ac parts of the signal be split, the following procedure is applied directly to the total voltage output of the CVA and gives the total velocity. In order to simulate an experimental data set and to test the robustness of the approach, a voltage output $\tilde{E}_{T_c}$ is constructed by adding a white noise of amplitude 1 mV rms to the E_{T_c} signal obtained in Sec. IV. Variables simulating an experimental data set are denoted hereafter by a tilde.

The instantaneous resistance of the real wire $\tilde{R}_w$ is computed from the measured voltage output $\tilde{E}_{T_c}$ using Eq. (1) for the electronic circuit of the CVA. Then, the thermal inertia of the wire is accounted for by Eq. (5) and the instantaneous resistance of the ideal wire $\tilde{R}_w^*$ is deduced from the resistance

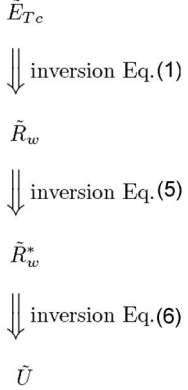

FIG. 4. Diagram of the present method for data processing.

of the real wire $\tilde{R}_w$. Finally, the instantaneous flow velocity $\tilde{U}$ is obtained from Eq. (6) using a heat transfer law or a calibration curve.

In the new procedure, only one factor $m_w c_w/\chi R_0$ is required in Eq. (5). This factor is a constant and it is advantageously deduced from the time constant M_w^{CVA}, which is usually measured. Indeed, Eq. (10) leads to

$$\frac{m_w c_w}{\chi R_0} = V_w^2 \frac{M_w^{\mathrm{CVA}}}{LM} \frac{1}{(\bar{R}_w + r_L)^2} \frac{1 + 2\bar{a}_w}{\bar{a}_w}. \tag{14}$$

Hence, altogether, the wire diameter, its length, as well as χ and c_w do not have to be known separately. As an example, using the wire characteristics and operating parameters given in Sec. IV, the factor $m_w c_w/\chi R_0$ is 0.39×10^{-5} s A^2. Moreover, an accurate measurement of M_w^{CVA} is possible in any nonturbulent flow prior to systematic turbulence investigations.

The calibration is done as usual in a very low turbulence flow such as the potential core of a jet or the free stream of a boundary layer. As T_c has no effect in that situation, the CVA output is that of an ideal wire. Hence, from Eq. (1),

$$E_{T_c}^* = V_w \left[1 + \frac{R_2}{R_F} + \frac{R_2}{R_w^* + r_L} \right], \tag{15}$$

or conversely,

$$R_w^* = R_2 \left[\frac{E_{T_c}^*}{V_w} - 1 - \frac{R_2}{R_F} \right]^{-1} - r_L. \tag{16}$$

The values of $E_{T_c}^*$ or R_w^* may be stored in a look-up table or as a polynomial fit to the calibration curve.

In practice, an experimental procedure may be organized as follows:

(1) Measure R_a, r_L, and estimate LM using Eq. (11).
(2) Choose V_w and T_c.
(3) Acquire and store the calibration curve using Eq. (15) or (16).
(4) Measure M_w^{CVA} *in-situ* or in a calibration facility and deduce $m_w c_w/\chi R_0$ using Eq. (14).
(5) Acquire $\tilde{E}_{T_c}$ in the turbulent flow to be investigated without changing T_c.
(6) Process the data by solving first Eq. (1) to obtain $\tilde{R}_w$ and then Eq. (5) to obtain $\tilde{R}_w^*$.

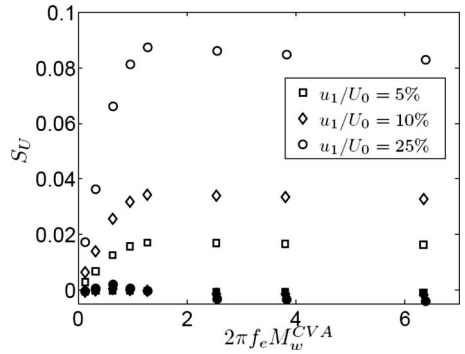

FIG. 5. Skewness factors obtained by the present method (filled symbols) and the best previous one (empty symbols), for different sinusoidal velocity inputs.

(7) Use Eq. (15) or (16) to deduce the instantaneous velocity $\tilde{U}$ from $\tilde{R}_w^*$.

VII. COMPARISON OF THE PRESENT METHOD TO THE BEST PREVIOUS ONE

Two examples are considered in order to compare the skewness factors of velocity signals obtained by the present method, i.e., $\tilde{U}$, and those obtained by the best previous method, i.e., $\hat{U}$.

The first example is a sinusoidal velocity signal for which a zero skewness is expected. Different amplitudes and different frequencies have been considered. Figure 5 reports the values that have been obtained. Clearly, only the present method permits the zero skewness to be recovered.

The second example deals more realistically with the velocity signals computed by large eddy simulation (LES) in a high-speed jet by Bogey and Bailly.[22] Along the jet axis, different downstream distances x have been chosen, $x/D=1$, 2, 3, 4, 6, and 8, where D is the diameter of the jet nozzle. Thus, different turbulence levels from low to high values may be considered. Every data set contains 15 000 velocity samples and the time interval is 10 μs. The heat-transfer law of the wire is approached by $Nu_d=0.56Re_d$ and the signal $\tilde{E}_{T_c}$ is constructed from E_{T_c} by adding a white noise of amplitude 1 mV rms. Results for the turbulence levels and the skewness factors are listed in Table III. Power spectral densities are presented in Fig. 6. Differences in turbulence levels and

TABLE III. Turbulence levels and skewness factors along the centerline of a high-speed jet (Ref. 22) obtained by the present method and the best previous one.

	RMS levels (%)			Skewness factors		
x/D	U LES	$\hat{U}$ Previous	$\tilde{U}$ Present	U LES	$\hat{U}$ Previous	$\tilde{U}$ Present
1	0.40	0.39	0.42	−0.009	−0.020	−0.009
2	1.70	1.58	1.71	−0.141	−0.115	−0.141
3	4.62	4.28	4.62	−0.104	−0.035	−0.106
4	6.59	6.10	6.59	−0.134	−0.022	−0.142
6	12.1	11.1	12.1	−0.557	−0.326	−0.567
8	12.6	11.8	12.7	−0.211	−0.021	−0.219

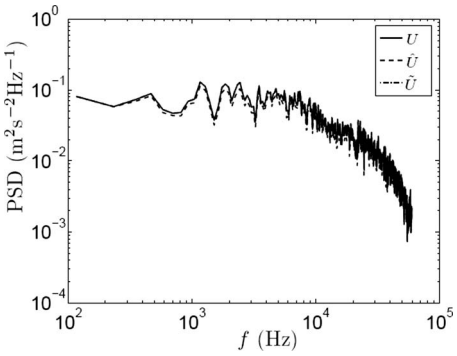

FIG. 6. Power spectral densities of the velocity on the jet axis ($x=6D$) obtained by the present method and by the best previous one compared to the LES simulation. The three spectra are almost superimposed.

spectra are negligible. For the skewness factors, only the values provided by the present method are in good agreement with the LES data.

VIII. CONCLUSIONS

The present procedure is much simpler than any of the previous ones and is exact at large-amplitude velocity fluctuations. It is based on the rational equations that govern the wire behavior and the electronic circuit of CVA without simplifications. All equations to be solved are easily implemented on a personal computer when postprocessing experimental data. Even if no differences appear between the previous method and the present one in turbulence levels and spectra, the use of the present method is compulsory when odd moments are to be investigated. The two major assets of the CVA, i.e., a constant bandwidth and an external fast and stable V_w command to correct for temperature drifts in the incident flow, remain valid. The present method has been validated for the case of a single-wire probe and may be easily extended to cross-wire probes and multiple-wire arrays.

ACKNOWLEDGMENTS

The authors are grateful to Christophe Bogey and Christophe Bailly for supplying the LES data and also to Dr. Siva Mangalam from Tao Systems Inc. for the loan of a CVA prototype. This work is supported by the French National Research Agency ANR (Project MicroThermAc NT051_42101).

[1] S. Corrsin, in *Handbuch der Physik*, edited by S. Flugge (Springer, Berlin, 1963), Vol. VIII/2, pp. 524–590.
[2] G. Comte-Bellot and J. P. Schon, Int. J. Heat Mass Transfer **12**, 1661 (1969).
[3] P. Freymuth, Rev. Sci. Instrum. **40**, 258 (1969).
[4] P. Freymuth, J. Phys. E **10**, 710 (1977).
[5] H. J. Hussein, S. P. Capp, and W. K. George, J. Fluid Mech. **258**, 31 (1994).
[6] H. H. Bruun, *Hot Wire Anemometry* (Oxford Scientific, UK, 1995).
[7] P. Ligęza, Rev. Sci. Instrum. **78**, 075104 (2007).
[8] G. R. Sarma, Rev. Sci. Instrum. **69**, 2385 (1998).
[9] G. Comte-Bellot, in *Handbook of Fluid Dynamics*, edited by R. W. Johnson (CRC, Boca Raton, FL, 1998), Chap. 34.
[10] G. Comte-Bellot, in *Handbook of Experimental Fluid Mechanics*, edited by C. Tropea, A. L. Yarin, and J. F. Foss (Springer, Berlin, 2007), pp. 229–283.
[11] G. Comte-Bellot, J. Weiss, and J. C. Béra, 58th Annual Meeting of the Division of Fluid Dynamics, Chicago, 20–22 November 2005 (unpublished), p. 189.
[12] G. R. Sarma, G. Comte-Bellot, and Th. M. Faure, Rev. Sci. Instrum. **69**, 3223 (1998).
[13] G. Comte-Bellot and G. R. Sarma, AIAA J. **39**, 261 (2001).
[14] J. D. Norris and N. Chokani, AIAA J. **41**, 1619 (2003).
[15] T. R. Moes, G. R. Sarma, and S. M. Mangalam, Flight demonstration of a shock location sensor using constant voltage hot-film anemometry, NASA Technical Memorandum 4806, 1997.
[16] G. Comte-Bellot, J. Weiss, and J. C. Béra, Rev. Sci. Instrum. **75**, 2075 (2004).
[17] G. R. Sarma and R. W. Lankes, Rev. Sci. Instrum. **70**, 2384 (1999).
[18] L. S. G. Kovasznay, J. Aeronaut. Sci. **20**, 657 (1953).
[19] M. V. Morkovin, Fluctuations and hot-wire anemometry in compressible flows, AGARdograph 24, 1956.
[20] J. Gaviglio, Int. J. Heat Mass Transfer **30**, 911 (1987).
[21] G. R. Sarma and G. Comte-Bellot, Rev. Sci. Instrum. **73**, 1313 (2002).
[22] C. Bogey and C. Bailly, Phys. Fluids **18**, 065101 (2006).